



# DATA SPLITS AND METRICS FOR METHOD BENCHMARKING ON SURGICAL ACTION TRIPLET DATASETS

A BENCHMARK STUDY

 **Chinedu Innocent Nwoye**  
ICube Laboratory  
University of Strasbourg, France  
nwoye@unistra.fr

 **Nicolas Padoy**  
IHU Strasbourg, France  
ICube, University of Strasbourg, CNRS, France  
npadoy@unistra.fr

April 12, 2022

## ABSTRACT

In addition to generating data and annotations, devising sensible data splitting strategies and evaluation metrics is essential for the creation of a benchmark dataset. This practice ensures consensus on the usage of the data, homogeneous assessment, and uniform comparison of research methods on the dataset. This study focuses on CholecT50, which is a 50 video surgical dataset that formalizes surgical activities as triplets of  $\langle \text{instrument}, \text{verb}, \text{target} \rangle$ . In this paper, we introduce the standard splits for the CholecT50 and CholecT45 datasets and show how they compare with existing use of the dataset. CholecT45 is the first public release of 45 videos of CholecT50 dataset. We also develop a metrics library, *ivtmetrics*, for model evaluation on surgical triplets. Furthermore, we conduct a benchmark study by reproducing baseline methods in the most predominantly used deep learning frameworks (PyTorch and TensorFlow) to evaluate them using the proposed data splits and metrics and release them publicly to support future research. The proposed data splits and evaluation metrics will enable global tracking of research progress on the dataset and facilitate optimal model selection for further deployment.

**Keywords** : Surgical activity recognition · Tool-tissue interaction · Action triplet · CholecT40 · CholecT45 · CholecT50

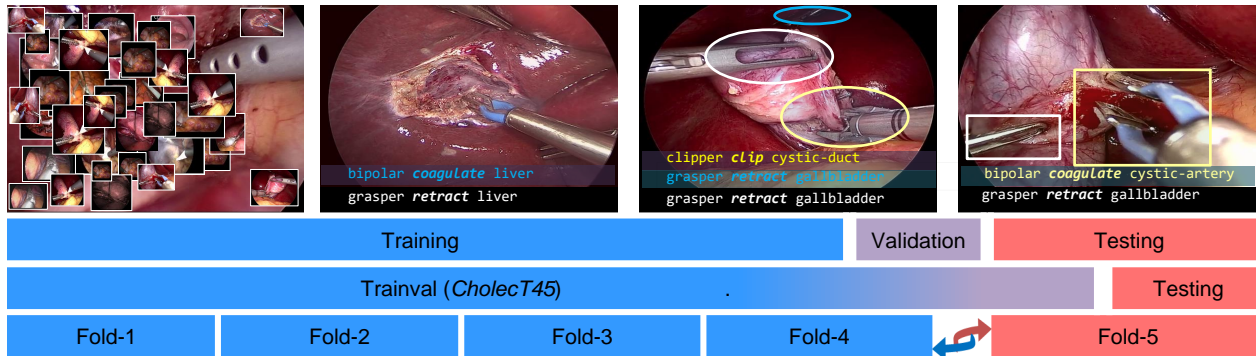


Figure 1: An illustration of the dataset splits. *Top*: CholecT50 split as used in the Rendezvous [1]. *Middle*: CholecT50 split as used in the CholecTriplet challenge [2]. *Bottom*: the official CholecT45 and CholecT50 cross-validation splits.

## 1 Introduction

The use of Artificial Intelligence (AI) techniques is increasingly driving research and development across many disciplines. Yet, there has been a delay in introducing large-scale data science to interventional medicine, partly due to the unavailability of large annotated datasets [3]. While huge efforts have been made in creating small to medium scale datasets [1, 4, 5, 6, 7, 8, 9, 10, 11], little or no effort has been made to standardize the data usage for tracking the global research progress. For instance, in laparoscopic and cataract surgeries, many published methods on the most prominent tasks of surgical phase [5, 12, 13, 14] and tool detection [15, 16, 17] are reported on varying data splits of the same dataset, e.g: Cholec80 [5], Cataract [7], etc. Without a consensus data split, tracking research progress on these experimental datasets is not straightforward. Oftentimes, it complicates results comparison, making model selection for further clinical translation more challenging.

In this paper, we present standard data splits for the recently introduced CholecT50 dataset [1]. The label formalism in the dataset provides comprehensive and fine-grained details on every tool-tissue interaction in any given surgical scene. A subset of the dataset, named *CholecT45*, was released after the CholecTriplet2021 challenge [2] while withholding 5 test set videos from public access. The remaining part of the dataset is planned to be released after the CholecTriplet2022 challenge.

The data split patterns, illustrated in Fig. 1, are fashioned on three criteria:

1. *Reproducibility*: to maintain consistent splits with the earlier published experiments that introduced the dataset,
2. *Accessibility*: owing that only a part of the dataset is publicly released to date, we consider a representative setup for its utilization and fair comparison,
3. *Thoroughness*: to counter the effect of class-imbalance predominant in a single test set by using a rigorous and exhaustive k-fold cross-validation approach, which enables alternating evaluation on the entire dataset.

Furthermore, we define and standardize the evaluation metrics for assessing the quality of triplet detection and recognition on the dataset. These metrics build on the evaluation setup used in earlier research [9, 18] on the dataset. In this work, we describe the evaluation algorithm and develop a standard metrics library, named *ivtmetrics*, for both triplet recognition and detection/localization evaluation. The metrics library is available online and can be installed via `pip` or `conda` package installers for method development and validation. The metrics library is usable in all python-based deep learning frameworks.

Finally, we re-implement our previously proposed deep learning methods for surgical action triplet recognition in two widely used deep learning frameworks: PyTorch and TensorFlow. The reproduced models are evaluated on the proposed data splits for CholecT45 and CholecT50 using the developed *ivtmetrics* library thus providing baselines for future comparison. By conducting this benchmark experiment on the newly introduced dataset, this study provides a definition of standard practice for the official data splits and an evaluation protocol to guide future research.

The CholecT45 dataset is released on <http://camma.u-strasbg.fr/datasets>. The evaluation metrics library is installable using python package and environment managers (`pip` and `conda`). The code and weights for the reproduced models are available on the CAMMA public GitHub <https://github.com/CAMMA-public>.

In the following sections, we present the proposed data splits and their constituting videos, followed by the evaluation protocols and the developed metrics library. Afterwards, we present the reproduced models, their performance across the proposed splits, and comprehensive per-category performance analysis on the two datasets.

## 2 Data Splits

CholecT50 [1] is a surgical dataset for action triplet recognition. It is an extension of CholecT40 dataset [9] with additional 10 videos. It contains 50 videos of laparoscopic cholecystectomy surgery annotated with 100 action triplet classes. Action triplet is a formalism to represent fine-grained activity in the form of  $\langle \text{instrument}, \text{verb}, \text{target} \rangle$ . In this dataset, they are composed from 6 instruments, 10 verbs, and 15 target classes resulting in over 161K triplet instances at 1 fps video frames.

In the CholecTriplet2021 [2] / CholecTriplet2022 challenges, the participants are given access to a subset of the CholecT50 dataset, also known as CholecT45. This subset is the first public release of the CholecT50 dataset available on <http://camma.u-strasbg.fr/datasets>. The videos of CholecT45 are part of the Cholec80 [5] dataset. The video indexes correspond between the two datasets with the prefix "video" in Cholec80 changed to "VID" in CholecT45. The statistics of the CholecT45 dataset is presented in Table 1

Table 1: Statistics of CholecT45 Dataset

Videos	Frames	Instances	Instruments	Verbs	Targets	Triples
45	90489	127385	6	10	15	100

Table 2: CholecT50 dataset split as used in Rendezvous publication [1].

Training							Validation	Testing	
VID01	VID15	VID26	VID40	VID52	VID65	VID79	VID08	VID06	VID51
VID02	VID18	VID27	VID43	VID56	VID66	VID92	VID12	VID10	VID73
VID04	VID22	VID31	VID47	VID57	VID68	VID96	VID29	VID14	VID74
VID05	VID23	VID35	VID48	VID60	VID70	VID103	VID50	VID32	VID80
VID13	VID25	VID36	VID49	VID62	VID75	VID110	VID78	VID42	VID111

To describe the official usage of CholecT45 and CholecT50 datasets, we present the different splits of the datasets in the following sections. We first present the data split of CholecT50 as used (a) in the Rendezvous paper [1] that introduces the dataset and (b) in the CholecTriplet challenges [2] for reproducibility. Afterward, we present the official cross-validation splits of the CholecT45 and CholecT50 datasets.

### 2.1 Rendezvous (RDV) Split of CholecT50 dataset

This split is used in the original paper [1] that introduces the dataset. It is presented for reproducibility of the earlier published methods on this task. In this setup, the dataset is split into three: (1) training, (2) validation, and (3) testing as presented in Table 2. The videos in each dataset split are distributed in the same ratio to include annotations from each of the (surgeon) annotators. This helps to minimize the effect of annotation bias on the learning algorithm.

### 2.2 CholecTriplet Split of CholecT50 dataset

This split is introduced by the organizers of the CholecTriplet2021 and CholecTriplet2022 challenges for surgical action triplet recognition and detection. Here, it is selected for consistency with the methods presented at the MICCAI 2021 EndoVis challenge. The dataset is split into two: (1) trainval, and (2) testing set, as presented in Table 3. During the challenge and for model hyper-parameter tuning, participants are allowed to further split the trainval split into training and validation subsets at their own discretion. All the videos in the trainval are drawn from the publicly available Cholec80 [5] dataset. Nevertheless, the testing set containing 5 videos are not in the public domain. The rationale for this data split is to ensure that the participants do not have access to the testing set of the challenge dataset for fairness in the competition.

### 2.3 Official Cross-Validation (CV) Splits for CholecT45 and CholecT50 datasets

$K$ -fold cross-validation is known for its robustness in result analysis. As some of the triplet classes can be unrepresented in any testing set sampling, cross-validation is a more robust, and stable way of assessing the quality of model predictions on all observed triplet classes. This enables a result analysis that covers all the 100 class labels of the triplet datasets. In this setup, the dataset is split into 5 equal subsets called *folds*. Different copies of a model are trained on different combinations of 4 out of 5 folds, each time leaving out one alternating fold for testing. The final result is averaged over the 5 hold-out testing splits.

To ensure that all folds have similar levels of complexity, the 50 videos of CholecT50 are sorted by their difficulty, determined by procedure duration. The sorted videos are divided into 10 clusters with each containing 5 videos of the same/similar complexity or duration. The videos in each cluster are randomly distributed to all the 5 folds split.

The **CholecT50 CV split** contains the full 50 video dataset divided into 5 folds with each fold containing 10 videos as presented in Table 4) (rows 1-10).

The **CholecT45 CV split**, on the other hand, contains 45 videos of the dataset divided into 5 folds with each fold containing 9 videos each as shown in Table 4) (rows 1-9). The CholecT45 excludes the test videos (row 10) of the CholecTriplet challenge. Hence, this split equally supports exhaustive cross-validation but only on the publicly released subset of the entire dataset.

Table 3: CholecT50 dataset split as used in CholecTriplet2021 [2] &amp; CholecTriplet2022 challenges.

Trainval (= <i>CholecT45</i> )									Testing
VID01	VID10	VID22	VID29	VID42	VID50	VID60	VID73	VID05	VID92
VID02	VID12	VID23	VID31	VID43	VID51	VID62	VID75	VID18	VID96
VID04	VID13	VID25	VID32	VID47	VID52	VID66	VID78	VID36	VID103
VID06	VID14	VID26	VID35	VID48	VID56	VID68	VID79	VID65	VID110
VID08	VID15	VID27	VID40	VID49	VID57	VID70	VID80	VID74	VID111

Table 4: Official cross-validation data splits of CholecT45 and CholecT50 datasets.

		Fold 1	Fold 2	Fold 3	Fold 4	Fold 5	
1	CholecT50 Cross-Val. splits	CholecT45 Cross-Val.	VID79	VID80	VID31	VID42	VID78
2			VID02	VID32	VID57	VID29	VID43
3			VID51	VID05	VID36	VID60	VID62
4			VID06	VID15	VID18	VID27	VID35
5			VID25	VID40	VID52	VID65	VID74
6			VID14	VID47	VID68	VID75	VID01
7			VID66	VID26	VID10	VID22	VID56
8			VID23	VID48	VID08	VID49	VID04
9			VID50	VID70	VID73	VID12	VID13
10			VID111	VID96	VID103	VID110	VID92

### 3 Metrics

#### 3.1 Recognition Average Precision

Triplet recognition performance is evaluated using the Average Precision (AP) metric measured as the area under the precision-recall ( $p$ - $r$ ) curve per class:

$$AP = \int_0^1 p(r) dr. \quad (1)$$

AP summarizes a  $p$ - $r$  curve as the weighted mean of precisions achieved at each threshold, with the increase in recall from the previous threshold used as the weight. Video-specific AP score for evaluating surgical action triplet recognition is computed as follows:

- i. *per-category AP* is computed across all frames in a given video.
- ii. *category AP* is obtained by averaging per-category APs across all videos.
- iii. *mean AP* is obtained by averaging  $N$  category AP, serving as the final score:

$$mAP = \frac{1}{N} \sum_{i=1}^N AP_i. \quad (2)$$

The same process is followed when computing mAP for the individual components of the triplets. The predictive capacity of a model at recognizing correctly a triplet and its components is evaluated in two ways:

1. **Component average precision:** This includes three APs assessing the correct recognition of the instrument ( $AP_I$ ), verb ( $AP_V$ ), and target ( $AP_T$ ) components of the triplets.
2. **Triplet average precision:** This includes three APs assessing the correct recognition of tool-tissue interactions by observing different sets of triplet components, which includes: APs for instrument-verb ( $AP_{IV}$ ), instrument-target ( $AP_{IT}$ ), and instrument-verb-target ( $AP_{IVT}$ ), which is the main metric.

#### 3.2 Disentangling Action Triplet Prediction

This is introduced to support the evaluation of all triplet component prediction for models that produce only the final triplet ( $Y_{IVT}$ ) probabilities. If  $IVT$  represents all the triplets in a single image, and  $D = \{I, V, T, IV, IT\}$  is a set of

the triplets' components and their possible combinations, then,  $\forall d \in D$ , the indirect component's output vector  $Y_d$  of class size  $C_d$  (e.g. for  $d = I$ ,  $C_d = 6$  as there are 6 instrument classes) can be filtered from  $Y_{IVT}$  following Equation 3:

$$Y_d = \left[ \max_{d^k \in \{i,v,t\}} Y_{ivt} \right] \quad \forall ivt \in IVT, k : 0 \leq k < C_d. \quad (3)$$

This filtering algorithm [1] directly translates to obtaining the probability of a given component class as the maximum probability value among all triplet labels having the same component class label in a video frame. Likewise, the groundtruths of the component labels can be obtained using the filtering setup.

### 3.3 Detection Average Precision

When evaluating the localization of the triplets as in CholecTriplet2022 challenge, AP metrics consider the overlap or Intersection of Union (IoU) of the predicted bounding boxes with the ground truth. The detection AP is evaluated in two ways:

1. **Instrument Localization AP:** In this metric, a detection is assigned a true positive (TP) if the degree of overlap between a predicted bounding box and the ground truth exceeds a certain threshold (usually 0.5) and the instrument ID is correct.
2. **Triplet Detection AP:** This metric assess the correctness of every associated action triplet to every localized instrument. Here, a prediction is considered a TP if the predicted triplet ID is correct, assigned to the right instrument involved in the tool-tissue interaction, which must also be localized at a minimum IoU threshold with the ground-truth bounding box.

The missed predictions are marked as false negatives (FN) whereas false alarms are marked as false positives (FP). Following this, their corresponding precision ( $p$ ) and recalls ( $r$ ) are calculated as follows:

$$\begin{aligned} p &= \frac{TP}{TP + FP}, \\ r &= \frac{TP}{TP + FN}, \end{aligned} \quad (4)$$

and using the computed  $p, r$ , the AP is calculated following Equation 1, averaged across videos.

In future, when *target localization AP* is considered, the triplet detection AP will take into account a satisfied bounding box IoU for both instruments and targets.

### 3.4 Metrics Library

To standardize the use of these evaluation metrics, we develop *ivtmetrics* library, which can be used in both training and inference mode. The library can be imported in a python-based script using `import ivtmetrics` with a prerequisite installation step: `pip install ivtmetrics` or `conda install -c nwoye ivtmetrics`. The library provides metrics classes for triplet recognition: `AP = ivtmetrics.Recognition(N : int)` and triplet detection `AP = ivtmetrics.Detection(N : int)`, as well as an internally implemented triplet component filtering `AP = ivtmetrics.Disentangle(N : int)`, where  $N$  = number of triplet classes. Invoking the metrics class initializes the metrics accumulators by a `AP.reset()`. This reset function is to be called at the beginning of every training epoch. Other reset options include `AP.reset_video()` to reset scores accumulated for all seen videos, and `AP.reset_global()` to reset every accumulator. The metrics update function takes in the predicted and target labels over each iteration by calling `AP.update(targets: array, predictions: array)`. If a video-specific AP is needed, `AP.video_end()` must be called at the end of each video. The AP scores from a current time up to the last `reset()` call are obtained via `AP.compute_AP(component : str)`. The mean AP average across videos is obtained by calling `AP.compute_video_AP(component : str)` while `AP.compute_global_AP(component : str)` gives the mean AP across all frames in all seen videos. The component  $\in$  ("i", "v", "t", "iv", "it", "ivt") is a string argument that describes the respective sub-task's (instrument, verb, target, instrument-verb, instrument-target, instrument-verb-target) performance to be computed for. A top  $K$  performance is obtained by `AP.topk(k : int)` while top predicted class IDs are given by `AP.topClass(k : int)`. More details and usage examples of the *ivtmetrics* can be found on GitHub <https://github.com/CAMMA-public/ivtmetrics>.

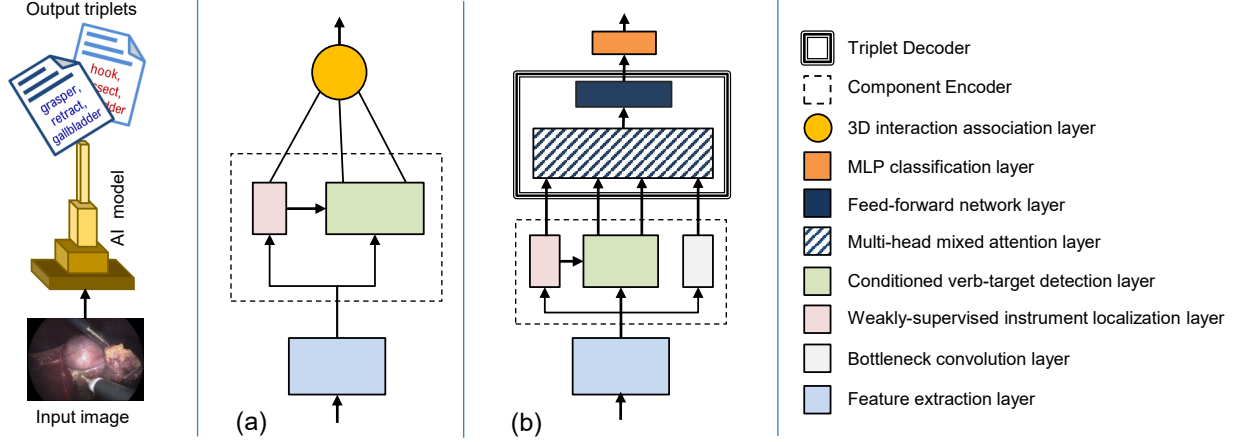


Figure 2: Reproduced models for surgical action triplet recognition: (a) Tripnet [9], (b) Rendezvous [1].

## 4 Benchmark Study Design

To provide a benchmark study on CholecT45 and CholecT50 datasets using our proposed data splits and metrics, we re-implement and reproduce three proposed methods in PyTorch and TensorFlow.

### 4.1 Methods

We summarize the reproduced methods as follows:

1. **Tripnet**: As shown in Fig. 2(a), Tripnet [9] is a multi-task learning method that uses activation maps resulting from the instrument branch to enhance verb and target feature encoding in a new module known as class activation guide (CAG). It is followed by a 3D interaction space where relationships between instruments-verbs-targets components are resolved to triplets. Code and weights are publicly released on GitHub <https://github.com/CAMMA-public/tripnet>.
2. **Attention Tripnet**: This is an upgrade of Tripnet with an attention mechanism. The main difference is the use of class activation guided attention mechanism (CAGAM) [1] over CAG where the verb and target feature discovery are obtained by channel and position attention processes respectively. Code and weights are publicly released on GitHub <https://github.com/CAMMA-public/attention-tripnet>.
3. **Rendezvous (RDV)**: In this model [1], the network encoder uses a weakly supervised approach to localize the instruments and the CAGAM module to detect the verb and target components of the triplets as shown in Fig. 2(b). The association part is achieved by both self and cross attention mechanisms in a new module known as multi-head of mixed attention (MHMA), and terminated by a simple classifier after 8 successive layers of association decoding. Code and weights are publicly released on GitHub <https://github.com/CAMMA-public/rendezvous>.

### 4.2 Implementation Details

We made few changes in the original implementations [1, 9] as follows:

1. **Output resolution**: The original implementation lowered the strides of the last two blocks of the ResNet by one pixel to provide higher resolution ( $32 \times 56$ ) output. However, using original strides of size 2, we implement a faster version (size:  $8 \times 14$ ), trading-off precise localization to speed.
2. **Attention normalization**: The huge parameter layer-norms in the AddNorm layers of the attention module are replaced with batch-norms without affecting model accuracy.
3. **Loss function**: We integrates warmup parameters within the auxiliary task' cross-entropies without requiring additional uncertainty loss balancing [19] as in [1]. This removes the excessive parameters introduced by the uncertainty loss.

## 5 Benchmark Results and Discussion

Table 5: Benchmark triplet recognition AP (%) on CholecT50 dataset for different frameworks using RDV split.

Framework	Method	Component detection			Triplet association		
		$AP_I$	$AP_V$	$AP_T$	$AP_{IV}$	$AP_{IT}$	$AP_{IVT}$
TensorFlow	Tripnet [9]	<b>92.1</b>	54.5	33.2	29.7	26.4	20.0
	Attention Tripnet [1]	92.0	60.2	38.5	31.1	29.8	23.4
	Rendezvous (RDV) [1]	92.0	60.7	38.3	39.4	<b>36.9</b>	<b>29.9</b>
PyTorch	Tripnet [9]	88.7	59.2	39.3	31.9	27.9	21.6
	Attention Tripnet [1]	87.9	59.7	40.6	34.2	29.0	23.2
	Rendezvous [1]	89.1	<b>62.3</b>	<b>43.8</b>	<b>40.0</b>	35.8	29.5

### 5.1 Quantitative Results on CholecT50 using Rendezvous Split

All the 100 triplet classes are evaluated in this setup. The benchmark results on the RDV split is presented in Table 5. The results follow the same trend as in the original paper [1] as it is observed that the Attention Tripnet leverages CAGAM to improve the verb and target detections while Rendezvous utilizes its transformer-inspired MHMA to improve the triplet association performance. We show the performance across deep learning frameworks in Table 5. The PyTorch models approximates the performance of their TensorFlow counterparts (version 1). We observe that these results are comparable in some of the sub tasks.

### 5.2 Quantitative Results on CholecT50 using CholecTriplet Split

The challenge rule excludes the 6 null triplet classes (IDs: 94-99) from evaluation. The results are presented in Table 6. It is observed that  $AP_{IVT}$  is higher than in the RDV split for each model, likely due to the reduced number of triplet classes (94 v 100). Also, the direct outputs ( $Y_D$ ) for the individual components (i.e.:  $Y_I, Y_V, Y_T, Y_{IV}$  or  $Y_{IT}$ ) of the triplets ( $Y_{IVT}$ ) are not provided by the challenge approaches, instead they are filtered from the main triplet predictions ( $Y_{IVT}$ ) following the filtering formula in Section 3.2. As shown in Table 6, the AP performances on the filtered prediction are generally lower compared to AP on directly predicted probabilities of those components when provided, however, they are more informative and a better representation of how a model understands the triplet’s composition.

Table 6: Benchmark triplet recognition AP (%) on CholecT50 dataset using CholecTriplet split.

Framework	Method	Component detection			Triplet association		
		$AP_I$	$AP_V$	$AP_T$	$AP_{IV}$	$AP_{IT}$	$AP_{IVT}$
TensorFlow	Tripnet [9]	74.6	42.9	32.2	27.0	28.0	23.4
	Attention Tripnet [1]	77.1	43.4	30.0	32.3	29.7	25.5
	Rendezvous [1]	<b>77.5</b>	<b>47.5</b>	37.7	34.4	<b>38.2</b>	32.7
PyTorch	Tripnet [9]	73.9	41.6	32.1	28.8	29.2	27.4
	Attention Tripnet [1]	73.7	43.7	35.3	31.6	31.9	27.7
	Rendezvous [1]	75.9	46.0	<b>38.7</b>	<b>35.9</b>	37.1	<b>32.8</b>

### 5.3 Quantitative Results on CholecT50 using Cross-Validation Split

The benchmarking results on the CholecT50 cross-validation split are presented in Table 7 along with the standard deviation (std) over the folds. All the 100 triplet classes are evaluated in this setup. This presents a less biased and less optimistic estimate of the models with confidence intervals. Their standard deviation (std) spread shows the extent of performances approximation of the three models positioning Tripnet as the least and Rendezvous as the best in terms of performance.

Table 7: Benchmark triplet recognition AP (%) on CholecT50 dataset using the official cross-validation split.

Method (in PyTorch)	Component detection			Triplet association		
	$AP_I$	$AP_V$	$AP_T$	$AP_{IV}$	$AP_{IT}$	$AP_{IVT}$
Tripnet [9]	89.1±1.7	58.8±3.1	38.4±1.3	32.7±2.4	29.0±0.8	25.3±2.4
Attention Tripnet [1]	88.7±1.3	<b>61.1±2.0</b>	<b>40.7±3.2</b>	33.1±2.7	30.3±1.6	27.2±2.9
Rendezvous [1]	<b>89.4±2.0</b>	60.4±2.8	40.3±2.2	<b>34.5±2.8</b>	<b>31.8±1.0</b>	<b>29.4±2.5</b>

#### 5.4 Quantitative Results on CholecT45 using Cross-Validation Split

Similarly, the benchmarking results on the CholecT45 cross-validation split, presented in Table 8, justifies the use of attention mechanisms for surgical action triplet recognition. The analysis shows that the results obtained on the CholecT45 CV approximates the ones of the CholecT50 CV in all the sub-tasks, justifying its use/sufficiency in the absence of the complete CholecT50 dataset.

Table 8: Benchmark triplet recognition AP (%) on CholecT45 dataset using the official cross-validation split.

Method (in PyTorch)	Component detection			Triplet association		
	$AP_I$	$AP_V$	$AP_T$	$AP_{IV}$	$AP_{IT}$	$AP_{IVT}$
Tripnet [9]	<b>89.9±1.0</b>	59.9±0.9	37.4±1.5	31.8±4.1	27.1±2.8	24.4±4.7
Attention Tripnet [1]	89.1±2.1	61.2±0.6	<b>40.3±1.2</b>	33.0±2.9	29.4±1.2	27.2±2.7
Rendezvous [1]	89.3±2.1	<b>62.0±1.3</b>	40.0±1.4	<b>34.0±3.3</b>	<b>30.8±2.1</b>	<b>29.4±2.8</b>

#### 5.5 Class-wise Performances of the Benchmark Models

We present the per-class performance for the triplet components (Tables 9 - 11) and their association (Table 12) recognition using the cross-validation dataset splitting strategy on both CholecT45 and CholecT50. We observe similar performance pattern across the two datasets in all classes of each sub task showing the reliability of cross-validation split approach in model evaluation.

On instrument presence detection, as shown in Table 9, grasper and hook are the most detected owing to their highest occurrence frequencies in the dataset. However, hook is a little better detected than grasper owing to its uniqueness unlike the grasper which sometimes share some similarities with clipper, bipolar and scissor. The scissors and irrigator, on the other hand, are the least detected likely due to their low occurrence distributions in the datasets.

Table 9: Per-class instrument presence detection AP (%) on cross-validation splits (Method in PyTorch)

Classes	CholecT45			CholecT50		
	Tripnet	Attention Tripnet	RDV	Tripnet	Attention Tripnet	RDV
grasper	96.5±0.4	96.4±0.7	96.6±0.6	96.4±0.7	96.5±0.6	96.6±0.6
bipolar	88.4±4.2	86.0±4.2	87.4±4.7	89.0±3.4	88.2±4.2	88.5±4.1
hook	97.5±1.6	97.1±1.3	97.4±1.5	97.5±1.3	97.3±1.3	97.6±1.3
scissors	80.3±6.0	79.6±8.4	78.4±5.4	82.8±4.9	81.3±5.8	82.6±6.5
clipper	91.2±3.9	90.1±3.9	90.9±3.8	89.6±5.6	89.8±5.8	89.9±5.0
irrigator	86.0±4.1	85.3±2.8	84.5±6.8	79.6±6.5	79.1±5.7	81.3±4.9
Mean	<b>89.9±1.0</b>	89.1±2.1	89.3±2.1	89.1±1.7	88.7±1.3	<b>89.4±2.0</b>

For the verb recognition, grasp, retract, dissect, coagulate, clip, cut, and aspirate are better detect above 50% at all time as shown in Table 10. This is due to their strong affinities with unique instrument classes. Pack and irrigate are very challenging to discriminate from the dominant verbs of their instruments namely retract and aspirate. Null action, being a compendium of unconsidered actions, is the least recognized verb.



Table 10: Per-class verb recognition AP (%) on cross-validation splits (Method in PyTorch)

Classes	CholecT45			CholecT50		
	Tripnet	Attention Tripnet	RDV	Tripnet	Attention Tripnet	RDV
grasp	70.5±5.8	60.5±9.9	69.8±3.7	67.1±3.4	66.1±5.4	68.3±3.0
retract	90.5±5.4	84.0±9.8	89.7±7.2	86.7±5.1	85.8±5.4	86.7±5.8
dissect	93.0±2.8	86.5±9.9	93.2±3.9	90.9±2.4	90.6±2.4	91.0±3.3
coagulate	67.2±6.1	56.5±9.9	68.7±5.5	67.9±5.0	68.5±6.2	69.7±6.1
clip	85.4±6.4	67.8±9.8	85.5±3.7	85.5±6.3	86.1±5.4	86.5±5.5
cut	70.5±9.1	57.7±9.9	72.0±4.8	74.9±3.4	72.3±6.1	74.9±7.6
aspirate	60.7±9.2	47.1±9.9	57.8±9.9	57.4±4.9	57.1±7.3	56.7±5.5
irrigate	29.6±8.2	17.4±9.7	25.7±5.8	27.6±9.4	25.4±7.9	25.1±9.2
pack	32.1±9.9	25.8±9.9	31.2±9.9	26.8±9.9	33.2±9.9	20.0±9.9
null-verb	23.0±2.4	21.1±5.0	24.0±4.1	24.5±1.8	25.5±4.0	24.9±2.6
Mean	59.9±0.9	61.2±0.6	<b>62.0±1.3</b>	58.8±3.1	<b>61.1±2.0</b>	60.4±2.8

The per-class target detection reveals the most interesting areas of improvement. The predominant targets such as gallbladder, liver, and specimen-bag are well detected above 70% as shown in Table 11. The main challenge comes in detecting tiny anatomical structures such as cystic-artery, peritoneum, cystic-plate, cystic-pedicle, etc. as against conspicuous structures such as liver, omentum, cystic-duct, fluid, etc. Some anatomies with no clear boundaries such as abdominal wall, cystic-artery, etc. are fairly detected.

Table 11: Per-class target recognition AP (%) on cross-validation splits (Method in PyTorch)

Classes	CholecT45			CholecT50		
	Tripnet	Attention Tripnet	RDV	Tripnet	Attention Tripnet	RDV
gallbladder	93.6±1.1	91.2±6.5	93.7±1.2	93.6±1.3	93.8±1.0	93.6±1.6
cystic-plate	11.6±3.9	10.1±2.0	11.0±3.5	11.1±2.2	11.2±2.7	09.9±3.3
cystic-duct	47.2±5.8	41.9±9.9	47.1±2.8	47.6±5.6	48.1±3.1	47.2±3.9
cystic-artery	31.9±3.7	29.6±9.7	31.2±2.2	35.0±4.7	34.6±2.8	35.6±4.6
cystic-pedicle	04.0±2.4	08.7±6.0	13.4±7.8	10.3±5.0	06.9±8.2	10.4±6.5
blood-vessel	08.4±5.6	15.6±9.9	06.7±6.2	12.7±9.9	23.5±9.9	18.7±9.9
fluid	58.4±9.2	48.9±9.9	58.0±9.9	56.3±5.1	54.5±6.8	57.0±5.1
abdominal-wall/cavity	30.0±4.6	20.4±9.9	25.9±7.2	25.7±3.4	28.5±5.0	31.3±9.9
liver	71.8±5.5	65.3±9.9	72.9±2.5	72.7±6.5	73.5±4.4	74.8±4.2
adhesion	04.2±0.3	13.9±3.3	07.2±0.5	05.2±0.0	33.3±9.9	11.3±2.8
omentum	46.7±8.6	44.4±9.9	48.0±9.9	45.8±8.0	45.8±9.9	46.2±9.9
peritoneum	17.7±5.5	24.1±9.9	26.6±4.5	19.5±9.9	28.8±9.9	25.7±8.1
gut	10.7±7.7	09.6±6.9	09.5±6.9	13.6±8.3	14.4±6.6	15.5±7.4
specimen-bag	85.8±2.5	70.1±9.9	84.4±1.2	85.5±1.8	84.1±1.3	84.6±1.2
null-target	22.8±2.3	21.1±5.4	23.5±4.1	24.5±2.1	25.5±3.9	25.2±2.6
Mean	37.4±1.4	<b>40.3±1.2</b>	40.0±1.4	38.4±1.3	<b>40.7±3.2</b>	40.3±2.2

A presentation of class-wise results of the complete 100 triplet classes is only possible using the cross-validation approach. As shown in Table 12, the models recognizes the most important triplets such as grasper retracting gallbladder or grasping specimen-bag, hook dissecting either gallbladder or omentum, bipolar coagulating liver, clipper clipping cystic-artery and -duct with scissors cutting the same, and irrigator aspirating fluid or irrigating the cystic-duct. The good performance on these specific triplets are expected from the models' high performance on their specific triplet component classes. Surprising, the irrigator rare use in dissecting cystic-pedicle is well detected by RDV model.

Table 12: Per-class triplet recognition AP (%) on cross-validation splits (Method in PyTorch)

Classes	CholecT45			CholecT50			classes	CholecT45			CholecT50		
	Tripnet	Attention Tripnet	RDV	Tripnet	Attention Tripnet	RDV		Tripnet	Attention Tripnet	RDV	Tripnet	Attention Tripnet	RDV
grasper,dissect,cystic-plate	01.5±0.3	01.5±0.4	02.2±1.2	03.3±3.4	01.7±0.8	01.9±0.1	hook,coagulate,cystic-plate	00.5±0.1	00.0±0.0	00.3±0.1	01.8±0.1	00.4±0.1	00.4±0.1
grasper,dissect,gallbladder	09.5±9.5	04.6±5.6	05.0±4.3	06.2±9.7	07.7±8.3	11.6±9.9	hook,coagulate,gallbladder	06.1±8.2	03.2±1.7	05.6±6.8	08.6±9.2	03.8±2.9	06.7±5.8
grasper,dissect,omentum	01.3±1.2	05.1±5.4	03.4±4.0	03.1±3.7	03.0±1.8	01.8±1.1	hook,coagulate,liver	01.9±1.2	02.5±2.1	07.5±4.8	05.7±4.1	04.0±2.9	06.1±4.2
grasper,grasp,cystic-artery	01.5±0.3	01.3±0.3	02.0±0.6	01.9±1.3	01.3±0.3	02.3±0.4	hook,coagulate,omentum	07.6±7.6	10.3±6.1	06.3±7.4	13.6±9.9	04.8±2.1	05.0±2.1
grasper,grasp,cystic-duct	07.9±4.9	12.8±6.5	20.8±9.9	08.0±5.8	07.4±3.1	18.7±9.9	hook,cut,blood-vessel	00.0±0.0	00.0±0.0	00.0±0.0	01.6±0.1	01.2±0.1	01.0±0.1
grasper,grasp,cystic-pedicle	05.2±1.9	20.1±0.1	02.8±0.8	13.5±9.9	02.2±0.2	24.0±9.9	hook,cut,peritoneum	00.0±0.0	00.0±0.0	00.0±0.0	07.3±0.1	05.2±0.1	03.4±0.1
grasper,grasp,cystic-plate	20.3±9.9	21.6±9.9	23.8±9.9	07.8±3.8	06.0±5.6	06.3±4.5	hook,dissect,blood-vessel	00.7±0.1	01.2±0.1	00.9±0.1	01.4±0.1	00.7±0.1	00.8±0.1
grasper,grasp,gallbladder	23.8±9.9	22.2±9.9	30.5±9.9	28.6±9.9	28.2±9.9	29.4±9.9	hook,dissect,cystic-artery	20.4±4.9	19.7±6.6	20.7±4.3	25.5±5.6	22.7±4.6	26.8±6.9
grasper,grasp,gut	00.4±0.1	00.9±0.1	00.3±0.1	02.1±2.3	00.7±0.6	01.1±0.4	hook,dissect,cystic-duct	37.4±4.4	38.7±3.6	39.1±3.1	37.8±5.5	42.5±2.9	38.6±3.8
grasper,grasp,liver	02.5±2.0	02.3±3.1	16.9±9.9	07.8±7.7	02.1±2.0	06.2±4.6	hook,dissect,cystic-plate	14.4±6.5	11.5±5.1	18.3±9.9	13.6±7.5	17.3±9.9	14.5±7.7
grasper,grasp,omentum	04.5±5.8	06.1±4.2	26.7±9.9	08.7±6.2	03.8±5.8	11.4±9.7	hook,dissect,gallbladder	78.7±2.6	78.3±3.6	78.3±2.2	77.5±4.4	77.8±4.9	77.3±4.2
grasper,grasp,peritoneum	09.2±9.9	04.2±4.7	03.0±2.4	12.3±9.9	17.0±9.9	15.1±9.9	hook,dissect,omentum	62.5±9.9	65.1±7.0	63.9±8.6	67.4±9.9	66.5±9.9	67.2±9.9
grasper,grasp,specimen-bag	85.3±2.3	85.7±1.9	84.5±1.1	85.3±1.3	85.2±1.4	84.9±1.4	hook,dissect,peritoneum	15.1±2.8	11.9±8.5	27.3±3.8	19.8±6.3	32.5±7.4	26.9±9.0
grasper,pack,gallbladder	30.9±9.9	33.9±9.9	35.2±9.3	28.4±9.9	37.2±7.5	28.2±6.9	hook,retract,gallbladder	14.8±9.9	17.0±5.8	23.8±9.9	17.9±9.9	17.0±8.6	21.3±9.9
grasper,retract,cystic-duct	26.9±0.1	00.0±0.0	45.0±0.1	24.1±0.1	21.9±0.1	38.7±0.1	hook,retract,liver	05.0±6.5	12.1±3.4	19.2±9.9	06.8±5.5	11.3±9.9	11.3±7.9
grasper,retract,cystic-pedicle	00.8±0.1	02.1±0.1	01.4±0.1	01.5±0.1	01.2±0.1	02.0±0.1	scissors,coagulate,omentum	00.8±0.1	04.0±0.1	01.1±0.1	03.1±0.1	00.8±0.1	01.4±0.1
grasper,retract,cystic-plate	16.0±9.9	15.9±1.1	17.8±1.3	14.7±7.1	24.7±9.9	15.9±8.7	scissors,cut,adhesion	07.9±0.1	12.4±0.1	10.4±0.1	06.1±0.1	13.8±0.1	11.8±0.1
grasper,retract,gallbladder	83.4±7.6	86.5±4.4	83.9±9.6	79.6±6.9	78.3±8.2	79.2±8.9	scissors,cut,blood-vessel	19.1±9.9	36.7±9.9	33.4±9.9	01.9±1.7	10.2±1.3	37.5±9.9
grasper,retract,gut	08.5±5.2	10.5±6.0	10.8±5.1	18.3±8.9	13.7±6.2	17.4±9.9	scissors,cut,cystic-artery	50.6±9.9	62.1±4.8	57.3±5.6	56.1±5.8	58.9±9.4	58.9±7.2
grasper,retract,liver	69.7±6.7	72.1±6.8	72.0±2.6	71.0±6.2	71.0±4.7	74.1±3.9	scissors,cut,cystic-duct	51.8±9.9	56.3±5.6	59.0±7.3	56.4±5.8	56.7±5.7	58.6±4.2
grasper,retract,omentum	44.9±9.9	43.0±9.9	45.5±9.9	42.1±9.9	42.6±9.9	47.9±9.9	scissors,cut,cystic-plate	01.5±1.6	16.0±2.5	22.9±6.1	25.5±9.9	09.3±4.3	48.5±9.9
grasper,retract,peritoneum	17.7±9.9	31.3±9.9	43.5±9.9	24.0±9.9	50.5±9.9	46.5±9.9	scissors,cut,liver	02.1±0.1	14.9±0.1	08.8±0.1	25.4±0.1	06.3±0.1	23.9±0.1
bipolar,coagulate,abdominal-wall-cavity	41.2±9.9	40.0±9.9	35.6±9.9	39.4±9.9	45.9±8.1	41.1±9.9	scissors,cut,omentum	01.9±0.1	00.0±0.0	07.9±0.1	04.9±5.5	01.7±0.8	21.0±9.9
bipolar,coagulate,blood-vessel	05.5±4.1	12.2±9.1	24.0±9.9	23.2±9.9	50.8±9.9	41.3±9.9	scissors,cut,peritoneum	02.7±0.1	07.4±0.1	42.9±0.1	02.8±0.1	04.2±0.1	23.4±0.1
bipolar,coagulate,cystic-artery	21.3±1.5	03.9±0.1	15.4±4.9	11.3±6.4	09.4±3.7	26.2±9.9	scissors,dissect,cystic-plate	00.4±0.1	00.4±0.1	02.0±0.1	00.5±0.1	00.6±0.1	00.8±0.1
bipolar,coagulate,cystic-duct	02.6±0.1	03.8±0.1	07.7±0.1	00.8±0.1	01.3±0.1	01.4±0.1	scissors,dissect,gallbladder	02.3±0.1	00.0±0.0	03.7±0.1	02.7±0.1	00.9±0.1	01.4±0.1
bipolar,coagulate,cystic-pedicle	27.6±9.9	36.9±9.9	45.5±9.9	32.2±9.9	32.3±9.9	50.0±9.9	scissors,dissect,omentum	04.5±0.1	15.8±0.1	06.6±0.1	08.3±0.1	04.7±0.1	48.4±0.1
bipolar,coagulate,cystic-plate	29.3±9.9	25.6±9.9	40.5±9.9	31.7±9.9	35.8±9.9	33.3±9.9	clipper,clip,blood-vessel	13.6±5.8	15.5±9.9	17.4±9.9	12.1±9.9	20.9±9.9	24.9±3.6
bipolar,coagulate,gallbladder	36.6±9.9	52.4±9.9	43.7±9.9	43.0±9.9	41.3±9.9	48.5±9.9	clipper,clip,cystic-artery	58.7±4.1	61.2±9.9	66.5±4.0	57.9±9.9	61.6±9.9	67.4±3.5
bipolar,coagulate,liver	77.6±7.4	79.7±5.9	78.2±6.8	79.8±4.5	79.7±7.6	80.9±7.8	clipper,clip,cystic-duct	65.2±9.3	70.0±5.7	70.7±6.1	68.6±6.4	70.6±8.2	73.0±8.9
bipolar,coagulate,omentum	33.3±9.9	42.8±9.9	37.0±9.9	49.5±9.9	44.7±9.9	46.9±9.9	clipper,clip,cystic-pedicle	03.5±0.1	05.2±0.1	26.8±0.1	12.5±0.1	00.6±0.1	00.8±0.1
bipolar,coagulate,peritoneum	08.3±0.1	00.0±0.0	22.5±0.1	10.3±6.6	61.7±9.9	33.2±9.9	clipper,clip,cystic-plate	02.4±0.9	12.0±4.3	16.3±9.1	10.7±8.3	16.3±9.9	19.9±9.9
bipolar,dissect,adhesion	07.0±0.1	00.0±0.0	05.1±0.1	07.8±0.1	02.0±0.1	07.9±0.1	irrigator,aspirate,fluid	58.9±9.9	57.3±3.0	57.4±9.9	57.7±4.4	56.0±5.5	58.9±3.6
bipolar,dissect,cystic-artery	07.0±5.1	29.8±9.9	22.3±9.9	15.8±9.9	20.3±9.9	32.5±9.9	irrigator,dissect,cystic-duct	04.7±0.1	00.0±0.0	18.1±0.1	13.3±0.1	11.8±0.1	04.5±0.1
bipolar,dissect,cystic-duct	25.9±9.9	25.9±3.5	08.9±4.5	07.3±5.7	18.0±9.9	22.9±9.9	irrigator,dissect,cystic-pedicle	18.8±0.5	39.5±9.9	60.6±9.9	36.3±9.9	52.0±9.9	51.0±5.4
bipolar,dissect,cystic-plate	04.5±1.9	08.7±0.1	03.5±1.3	16.6±9.9	05.2±2.7	19.1±1.7	irrigator,dissect,cystic-plate	01.2±0.1	02.5±0.1	02.0±0.1	00.4±0.1	04.3±0.1	02.2±0.1
bipolar,dissect,gallbladder	23.0±9.9	39.3±9.9	20.5±6.3	12.2±9.9	20.0±9.9	19.5±9.9	irrigator,dissect,gallbladder	02.3±0.2	11.1±7.5	19.6±9.9	03.0±0.3	05.2±6.5	11.4±3.8
bipolar,dissect,omentum	11.0±0.1	00.0±0.0	26.0±0.1	09.2±0.1	53.2±0.1	33.0±0.1	irrigator,dissect,omentum	03.4±3.4	13.5±9.9	08.8±4.1	04.2±5.0	13.3±9.9	11.8±7.7
bipolar,grasp,cystic-plate	00.8±0.1	00.3±0.1	00.5±0.1	00.6±0.1	00.3±0.1	00.5±0.1	irrigator,irrigate,abdominal-wall-cavity	23.0±9.9	17.8±9.9	28.2±5.8	26.3±9.9	28.8±6.3	25.1±9.9
bipolar,grasp,liver	03.4±0.1	95.5±0.1	15.2±0.1	21.2±0.1	99.5±0.1	29.8±0.1	irrigator,irrigate,cystic-pedicle	92.4±2.6	96.1±6.0	92.8±2.0	94.0±4.6	91.1±0.6	01.8±0.8
bipolar,grasp,specimen-bag	23.3±9.9	25.6±9.9	26.7±9.9	17.0±9.9	23.7±9.9	16.6±9.9	irrigator,irrigate,liver	13.3±9.9	26.9±9.9	18.0±8.0	21.1±7.9	19.5±8.3	21.6±7.7
bipolar,retract,cystic-duct	00.2±0.1	00.2±0.1	01.7±0.1	00.2±0.1	00.3±0.1	01.4±0.1	irrigator,retract,gallbladder	19.1±9.9	21.9±9.9	48.5±9.9	42.8±9.9	07.1±6.1	33.3±9.9
bipolar,retract,cystic-pedicle	00.8±0.1	37.6±0.1	38.2±0.1	00.5±0.1	01.4±0.1	07.3±0.1	irrigator,retract,liver	16.7±3.2	24.7±9.9	27.5±6.0	15.2±6.1	21.7±9.9	24.5±4.9
bipolar,retract,gallbladder	01.0±0.2	01.9±1.5	01.7±0.7	00.8±0.5	03.5±2.8	18.0±9.9	irrigator,retract,omentum	05.1±6.7	02.8±2.7	11.0±9.9	06.8±7.2	23.6±9.9	03.2±1.9
bipolar,retract,liver	15.7±9.9	11.0±5.4	13.3±6.5	13.4±4.3	12.4±5.2	12.9±6.0	grasper,null-verb,null-target	22.6±4.8	23.0±9.9	24.4±5.6	24.5±3.2	25.2±4.1	24.6±3.5
bipolar,retract,omentum	05.6±4.6	14.8±6.7	17.1±9.4	20.4±8.4	21.6±9.9	17.9±4.2	bipolar,null-verb,null-target	13.0±4.0	14.8±7.7	14.0±7.4	16.6±9.9	14.5±8.0	19.0±9.9
hook,coagulate,blood-vessel	01.2±1.3	00.5±0.1	01.7±1.4	01.0±0.6	01.9±2.7	01.6±1.8	hook,null-verb,null-target	15.8±4.6	17.5±2.3	17.0±2.7	17.4±1.9	18.0±4.3	19.7±1.7
hook,coagulate,cystic-artery	00.5±0.1	00.6±0.1	01.3±0.1	00.8±0.1	01.3±0.1	00.4±0.1	scissors,null-verb,null-target	06.8±2.5	23.9±9.9	15.1±9.9	15.4±9.5	18.4±8.7	18.2±9.9
hook,coagulate,cystic-duct	02.6±3.7	00.5±0.5	02.8±1.8	01.4±1.1	01.6±1.4	05.1±7.3	clipper,null-verb,null-target	25.4±9.9	22.6±9.9	33.0±9.9	15.9±8.5	20.4±8.7	24.9±9.9
hook,coagulate,cystic-pedicle	00.9±0.4	00.5±0.2	05.6±7.5	01.3±1.3	00.7±0.4	00.5±0.1	irrigator,null-verb,null-target	15.2±9.0	14.7±6.6	13.1±3.8	16.4±8.6	16.8±9.2	14.0±8.9
Mean								24.4±04.7	27.2±02.7	<b>29.4±02.8</b>	25.3±02.4	27.2±02.9	<b>29.4±02.5</b>

## 6 Conclusion

With the public release of the CholecT45 dataset to support research on surgical action triplet recognition, we present in this paper a standard practice for splitting the dataset to enable a uniform comparison of research methods. These splits will remain relevant in the planned future release of the entire CholecT50 dataset. We also design, implement, and publicly release a python packaged metrics library, *ivtmetrics* for the evaluation of surgical action triplet recognition and localization on the dataset. For the benchmark study, we re-implement the current state-of-the-art models in two predominant deep learning frameworks, PyTorch and TensorFlow, and then train and evaluate them on the proposed data splits. Owing to the well-articulated rationale for dataset splits and exhaustive cross-validation, results obtained reflect better the generalization capability of the models. This study sets a rich foundation for fair comparison of methods researched on the CholecT45 and CholecT50 datasets using the same data splits and metrics. Future work will extend the metrics library to include more statistical evaluations.

## Acknowledgements:

This work was supported by French state funds managed within the Investissements d’Avenir program by BPI France (project CONDOR) and by the ANR under references ANR-11- LABX-0004 (Labex CAMI), ANR-16-CE33-0009 (DeepSurg), ANR-10-IAHU-02 (IHU Strasbourg) and ANR-20-CHIA-0029-01 (National AI Chair AI4ORSafety). It was granted access to the HPC resources of Unistra Mesocentre and GENCI-IDRIS (Grant 2021-AD011011638R1). The authors also thank the IHU and IRCAD research teams for their help with the initial data annotation during the CONDOR project.

## References

- [1] C. I. Nwoye, T. Yu, C. Gonzalez, B. Seeliger, P. Mascagni, D. Mutter, J. Marescaux, and N. Padoy, “Rendezvous: Attention mechanisms for the recognition of surgical action triplets in

- endoscopic videos,” *Medical Image Analysis*, vol. 78, p. 102433, 2022. [Online]. Available: <https://www.sciencedirect.com/science/article/pii/S1361841522000846>
- [2] C. I. Nwoye, D. Alapatt, T. Yu, A. Vardazaryan, F. Xia, Z. Zhao, ..., and N. Padoy, “Cholectriplet2021: a benchmark challenge for surgical action triplet recognition,” *arXiv preprint*, 2022.
  - [3] L. Maier-Hein, S. Vedula, S. Speidel, N. Navab, R. Kikinis, A. Park, M. Eisenmann, H. Feussner, G. Forestier, S. Giannarou *et al.*, “Surgical data science: Enabling next-generation surgery,” *Nature Biomedical Engineering*, vol. 1, pp. 691–696, 2017.
  - [4] R. Sznitman, K. Ali, R. Richa, R. H. Taylor, G. D. Hager, and P. Fua, “Data-driven visual tracking in retinal microsurgery,” in *International Conference on Medical Image Computing and Computer-Assisted Intervention*. Springer, 2012, pp. 568–575.
  - [5] A. P. Twinanda, S. Shehata, D. Mutter, J. Marescaux, M. De Mathelin, and N. Padoy, “Endonet: a deep architecture for recognition tasks on laparoscopic videos,” *IEEE transactions on medical imaging*, vol. 36, pp. 86–97, 2016.
  - [6] A. Jin, S. Yeung, J. Jopling, J. Krause, D. Azagury, A. Milstein, and L. Fei-Fei, “Tool detection and operative skill assessment in surgical videos using region-based convolutional neural networks,” in *2018 IEEE Winter Conference on Applications of Computer Vision (WACV)*. IEEE, 2018, pp. 691–699.
  - [7] H. Al Hajj, M. Lamard, P.-H. Conze, S. Roychowdhury, X. Hu, G. Maršalkaitė, O. Zisimopoulos, M. A. Dedmari, F. Zhao, J. Prellberg *et al.*, “Cataracts: Challenge on automatic tool annotation for cataract surgery,” *Medical image analysis*, vol. 52, pp. 24–41, 2019.
  - [8] M. Grammatikopoulou, E. Flouty, A. Kadkhodamohammadi, G. Quellec, A. Chow, J. Nehme, I. Luengo, and D. Stoyanov, “Cadis: Cataract dataset for image segmentation,” *arXiv preprint arXiv:1906.11586*, 2019.
  - [9] C. I. Nwoye, C. Gonzalez, T. Yu, P. Mascagni, D. Mutter, J. Marescaux, and N. Padoy, “Recognition of instrument-tissue interactions in endoscopic videos via action triplets,” in *International Conference on Medical Image Computing and Computer-Assisted Intervention*, 2020, pp. 364–374.
  - [10] T. Ross, A. Reinke, P. M. Full, M. Wagner, H. Kenngott, M. Apitz, H. Hempe, D. M. Filimon, P. Scholz, T. N. Tran *et al.*, “Robust medical instrument segmentation challenge 2019,” *arXiv preprint arXiv:2003.10299*, 2020.
  - [11] V. S. Bawa, G. Singh, F. KapingA, I. Skarga-Bandurova, E. Oleari, A. Leporini, C. Landolfo, P. Zhao, X. Xiang, G. Luo *et al.*, “The saras endoscopic surgeon action detection (esad) dataset: Challenges and methods,” *arXiv preprint arXiv:2104.03178*, 2021.
  - [12] O. Dergachyova, D. Bouget, A. Huauilmé, X. Morandi, and P. Jannin, “Automatic data-driven real-time segmentation and recognition of surgical workflow,” *International journal of computer assisted radiology and surgery*, vol. 11, no. 6, pp. 1081–1089, 2016.
  - [13] X. Gao, Y. Jin, Y. Long, Q. Dou, and P.-A. Heng, “Trans-svnet: Accurate phase recognition from surgical videos via hybrid embedding aggregation transformer,” *arXiv preprint arXiv:2103.09712*, 2021.
  - [14] I. Funke, A. Jenke, S. T. Mees, J. Weitz, S. Speidel, and S. Bodenstedt, “Temporal coherence-based self-supervised learning for laparoscopic workflow analysis,” in *OR 2.0 Context-Aware Operating Theaters, Computer Assisted Robotic Endoscopy, Clinical Image-Based Procedures, and Skin Image Analysis*, 2018, pp. 85–93.
  - [15] L. C. Garcia-Peraza-Herrera, W. Li, L. Fidon, C. Gruijthuijsen, A. Devreker, G. Attilakos, J. Deprest, E. Van-der Poorten, D. Stoyanov, T. Vercauteren *et al.*, “Toolnet: holistically-nested real-time segmentation of robotic surgical tools,” in *2017 IEEE/RSJ International Conference on Intelligent Robots and Systems (IROS)*. IEEE, 2017, pp. 5717–5722.
  - [16] A. Vardazaryan, D. Mutter, J. Marescaux, and N. Padoy, “Weakly-supervised learning for tool localization in laparoscopic videos,” in *Intravascular Imaging and Computer Assisted Stenting and Large-Scale Annotation of Biomedical Data and Expert Label Synthesis*, 2018, pp. 169–179.
  - [17] C. I. Nwoye, D. Mutter, J. Marescaux, and N. Padoy, “Weakly supervised convolutional lstm approach for tool tracking in laparoscopic videos,” *International journal of computer assisted radiology and surgery*, vol. 14, no. 6, pp. 1059–1067, 2019.
  - [18] C. I. Nwoye, “Deep learning methods for the detection and recognition of surgical tools and activities in laparoscopic videos,” Ph.D. dissertation, Université de Strasbourg, 2021. [Online]. Available: <http://icube-publis.unistra.fr/8-Nwoy21>
  - [19] A. Kendall, Y. Gal, and R. Cipolla, “Multi-task learning using uncertainty to weigh losses for scene geometry and semantics,” in *Proceedings of the IEEE conference on computer vision and pattern recognition*, 2018, pp. 7482–7491.